sustainability

MDPI

Article

Application of Magnesium Oxide for Metal Removal in Mine Water Treatment

Andrés Navarro [1,*] and María Izabel Martínez da Matta [2]

[1] Fluid Mechanics, Universitat Politècnica de Catalunya (UPC), Jordi Girona, 08034 Barcelona, Spain
[2] Faculty of Biology, University of Barcelona, 08007 Barcelona, Spain
* Correspondence: andres.f.navarro@upc.edu; Tel.: +34-937-398-151; Fax: +34-937-398150

Abstract: In this study low-grade magnesium oxide (MgO) produced by calcinations of natural magnesite was used in mine water treatment using a laboratory-column device. The treatment of mine water from the abandoned Osor mine (NE Spain) with MgO showed the removal of metals from both mine water and tailing leachates. The PHREEQC numerical code and the Geochemist's Workbench code (GWB) were used to evaluate the speciation of dissolved constituents and calculate the saturation state of the effluents. The analysis of the treated mine water showed the removal of As (from 1.59 to 0.31 µg/L), Cd (from 1.98 to <0.05 µg/L), Co (from 19.1 to <0.03 µg/L), F (from 2730 to 200 µg/L), Mn (from 841 to 0.6 µg/L), Ni (from 17.9 to <2 µg/L, U (from 9.16 to 0.08 µg/L), and Zn (from 2900 to 68.5 µg/L). Pb was also removed (from 98 to 35.2 µg/L) in the treatment of contaminated leachates from the mine waste. The mixing of MgO and water at room temperature may promote the formation of a stabilizing agent composed of hydroxides, carbonates, and magnesium-silicate-hydrates (MSH), which may remove Cd, Zn, and similar metals by sorption on MSH, substitution on the MSH lattice, and precipitation or co-precipitation with some of the hydrated phases.

Keywords: magnesium oxide; mine water treatment; circum-neutral mine water; geochemical modeling; metals; column test; leaching; PHREEQC

Citation: Navarro, A.; Martínez da Matta, M.I. Application of Magnesium Oxide for Metal Removal in Mine Water Treatment. *Sustainability* **2022**, *14*, 15857. https://doi.org/10.3390/su142315857

Academic Editor: Giehyeon Lee

Received: 6 October 2022
Accepted: 21 November 2022
Published: 28 November 2022

1. Introduction

Although mine water treatment is often focused on acid drainage, metals such as arsenic, cobalt, molybdenum, nickel, antimony, and zinc are soluble at near-neutral pH and can contaminate soil, surface waters, and groundwater even under non-acidic conditions [1–5]. Neutral mine drainage occurs when sufficient neutralization potential of rocks and/or tailings reacts and consumes acid in the waters that have been in contact with the sulfides or when sulfide oxidation is weak due to the low sulfide content in ore and/or mine waste [6–9]. The main hydrochemical reactions for circum-neutral mine water (CNMW) occurrence are shown in Equations (1)–(6) and are associated with sulfide oxidation and carbonate dissolution [5,10,11]:

(1) Pyrite and sphalerite oxidation.

$$FeS_2 + 7/2\ O_2 + H_2O \rightarrow Fe^{2+} + 2SO_4{}^{2-} + 2\ H^+ \quad (1)$$

$$ZnS + 2\ O_2 \rightarrow Zn^{2+} + SO_4{}^{2-} \quad (2)$$

(2) Calcite dissolution.

$$CaCO_3 + H^+ = Ca^{2+} + HCO_3{}^- \ (pH > 6.4) \quad (3)$$

$$CaCO_3 + 2H^+ = Ca^{2+} + H_2CO_3 \ (pH < 6.4) \quad (4)$$

The presence of some cations, such as Na, Mg, and K, in high concentrations in mine water may be associated with the weathering of some silicates (albite and muscovite) and may also explain the detection of high pH. The progression of the feldspar alteration

reactions changes the activities of the dissolved solutes: Ca^{2+}, Na^{+}, K^{+}, H^{+}, $SiO_2(aq)$; therefore. albite and other aluminosilicates detected are not stable in these waters and should dissolve:

(3) Silicate (albite) dissolution.

$$2NaAlSi_3O_8 + 2H^+ + 9H_2O \rightarrow 2Na^+ + Al_2Si_2O_5(OH)_4 + 4H_4SiO_4 \quad (5)$$

$$NaAlSi_3O_8 + H^+ + H_2O \rightarrow Na^+ + Al(OH)_3 + 3H_4SiO_4 \quad (6)$$

Mine drainage from abandoned surface and underground mines may be treated in several ways, including active technologies (requiring dedicated professional teams and control systems) and passive remediation systems [12–16]. Most mine water treatment technologies are associated with the removal of metals from "acid mine water" (AMD) using active, passive or semi-passive systems [12–18]. However, there are relatively few studies of CNMW treatment [19,20].

The use of magnesium oxide as an alternative to lime and caustic soda for hydroxide precipitation has been proposed in some studies. However, its cost is a disadvantage since it is approximately three times the cost of hydrated lime [21]. Nonetheless, the use of caustic magnesia (by-product of MgO production through the calcination of $MgCO_3$) may be useful in the attenuation of metals such as Cu, Mn, and Zn [17]. Significant reduction in metal concentration were obtained after using MgO to treat effluents with high concentrations of Zn (50 mg/L), Cu (10 mg/L), Al (20 mg/L), Fe (360 mg/L), and SO_4^{2-} (960 mg/L) that were associated with brucite dissolution [17]. Metal removal may be linked to co-precipitation reactions of metals with amorphous Fe and Al oxy-hydroxides. Thus, iron in the ferric state as well as other metals should readily precipitate as oxyhydroxide compounds in mine water with high Fe concentrations [18]:

$$Fe^{3+} + 2OH^- \rightarrow FeOOH + H^+ \quad (7)$$

Additionally, aluminum removal may be associated with the precipitation of $Al(OH)_3$. However, this species can redissolve when pH increases to 8.5 [18]:

$$Al^{3+} + 3OH^- \rightarrow Al(OH)_3 \quad (8)$$

$$Al(OH)_3 + OH^- \rightarrow [Al(OH)_4]^- \quad (9)$$

Likewise, MgO from caustic magnesia has been used to remove metals from contaminated groundwater and water contaminated with metals and Cr (VI) [22–25]. The removal of Ni (II) from wastewater was found by adsorption using globular magnesium oxide [26]. Moreover, AMD treatment with magnesite and MgO showed the decrease of As, Cd, Cr, Zn, Ni, and Mn in the treated mine water [27,28]. Tailings amended with magnesium oxide and other binders were more highly buffered and resistant against anthropogenic re-acidification than other tailings amended with conventional reactive materials [29,30]. In the treatment of contaminated soils by solidification/stabilization techniques, the use of MgO may reduce the leachability of some metals, specially Pb and Zn [31,32]. Additionally, MgO mixed with cementitious materials or Si-rich minerals has been used as a binder in the treatment of contaminated sediments [33,34].

The PHREEQC geochemical model uses solution equilibrium models to calculate aqueous speciation and saturation state of mineral phases, among other possibilities, and has been applied to evaluate the removal of heavy metals from lab-scale experiments with MgO [22,23]. Additionally, PHREEQC code is used in the study of AMD treatment by membrane technology and Zn and Ni removal from mine water using limestone treatment [35–38]. In the treatment of AMD and CNMW, PHREEQC is used in order to predict the mineral phases involved in sulfate removal [39]. Likewise, PHREEQC showed the removal of metals from mine water treated with magnesite which precipitated and formed oxy-hydroxysulfates, hydroxides, gypsum, and dolomite [40]. In addition, PHREEQC is

used to understand the geochemical processes in mine water treatment plants and dynamic modeling using the chemical reaction module [41–43] and to study the use of thermal activated non-cryptocrystalline magnesite on the treatment of AMD [44].

The overall objectives of this study were to investigate the potential use of MgO in passive mine water treatment, especially in the CNMW treatment, where the laboratory-column studies may be a novelty contribution in the mine water treatment. Additionally, the study evaluated the possible mechanisms of metal removal using the PHREEQC geochemical model. The PHREEQC code calculated the speciation and saturation index of the possible mineral phases which may control the mass transfer processes. Geochemical modeling may be a cost effective way for assessing the appropriate treatment processes for particular mine water.

2. Materials and Methods

2.1. Characterization of MgO

The low-grade MgO used in this study was produced by calcination in a rotary kiln of natural magnesite (Figure 1). The temperature of the calcination ranged from 500 °C to 1300 °C. The rotary kiln was 81 m in length and the magnesite remained inside of it for approximately 6 h. The MgO obtained under these conditions is termed "hard-burned" and shows a narrow range of reactivity. This grade is typically used when slow degradation or chemical reactivity is required, as is the case with animal feeds and fertilizers [22].

(**A**)

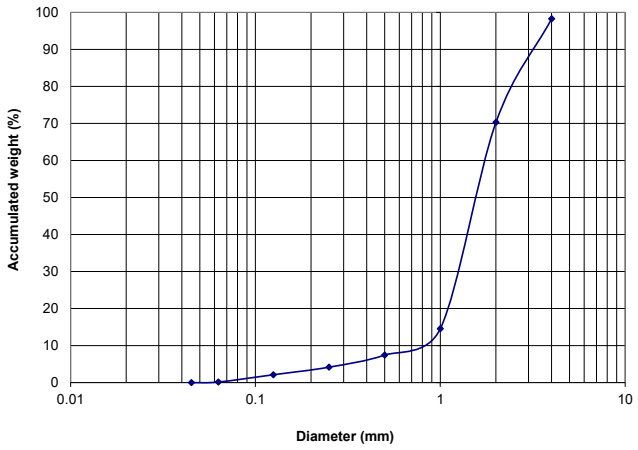

(**B**)

Figure 1. *Cont.*

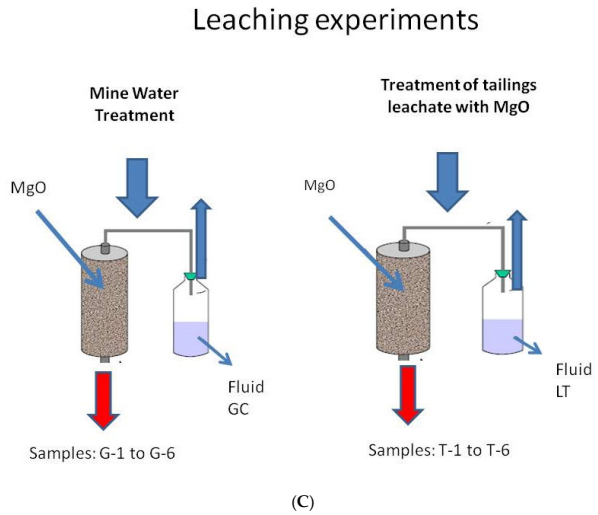

(**C**)

Figure 1. MgO characteristics. (**A**): MgO used in the experiments. (**B**): Grain size distribution of the MgO sample determined by an analytic sieve shaker (RETSCH model AS200). (**C**): Characteristics of column leaching experiments.

The MgO used in the experiments is a solid waste by-product projected to be reused as a metal adsorbent in treatment of mine water drainage or tailings remediation leachates. Additionally, the following physical characteristics of MgO were evaluated: pore size distribution, porosity, field capacity, and bulk density. Particle size distribution was determined by sieve analysis (RETSCH AS 200) using the following aperture ranges: 4, 2, 1, 0.5, 0.25, 0.125, 0.063, and 0.045 mm.

2.2. Geochemistry of MgO and Mine Wastes

The geochemical composition was analyzed using instrumental neutron activation analysis (INAA) and ICP-AES (inductively coupled plasma atomic emission spectrometry) in Actlabs (Ontario, Canada). The following elements were quantified by INAA: Au, Ag, As, Ba, Br, Ca, Co, Cr, Cs, Fe, Hf, Hg, Ir, Mo, Na, Ni, Rb, Sb, Sc, Se, Sn, Sr, Ta, Th, U, W, Zn, La, Ce, Nd, Sm, Eu, Tb, Yb, and Lu. In addition, the concentrations of the following elements were determined by acid digestion (employing HF, $HClO_4$, HNO_3 and HCl) and subsequent analysis by ICP-AES: Ag, Cd, Cu, Mn, Mo, Ni, Pb, Zn, Al, Be, Bi, Ca, K, Mg, P, Sr, Ti, V, Y, and S (Table 1). The grain size distribution of mine wastes was determined by sieving (RETSCH AS 200), the porosity by water displacement in a test tube due to their sandy character [23], and the field capacity by numerical methods.

Table 1. Composition of Osor tailings (TAL), ore sample, and MgO. CAL (*): The Catalonian soil intervention values (industrial use). ND: not determined. Data for Osor tailings and ore from [5].

Element	Al	Ag	As	Au	Ba	Be	Bi	Ca	Cd	Co	Cr	Cu	Fe	Hg	K	Mg	Mn	Mo	Na
Unit	%	ppm	ppm	ppb	ppm	ppm	ppm	%	ppm	ppm	ppm	ppm	%	ppm	%	%	ppm	ppm	%
Detection limit	0.01	0.3	0.01	2	50	1	2	0.01	0.3	0.1	0.3	1	0.01	0.05	0.01	0.01	1	0.05	0.01
Osor tailings (TAL)	4.46	0.6	12.5	<2	5110	2	0.3	7.33	7.6	14	39	47	1.78	<1	1.86	0.49	684	1	1.0
Osor ore	0.24	66.2	164	32	2190	1	<2	21.4	68.5	15	119	88	0.96	5	0.43	0.08	109	1	0.14
MgO	0.42	<0.3	17.5	<2	<50	<1	<2	7.07	<0.3	47	95	28	2.16	<1	0.30	32.6	965	<1	0.08
CAL *	—	—	30	—	1000	90	—	—	55	90	1000	1000	—	30	—	—	—	70	—

Element	Ni	P	Pb	Rb	S	Sb	Se	Sr	Ta	Ti	Th	U	V	W	Zn	La	Ce
Unit	ppm	%	ppm	ppm	%	ppm	ppm	ppm	ppm	%	ppm	ppm	ppm	ppm	ppm	ppm	ppm
Detection limit	1	0.001	1	1	0.01	0.005	0.1	1	0.5	0.01	0.1	0.01	2	0.05	1	0.01	0.1
Osor tailings (TAL)	18	0.041	940	103	0.23	1	<0.1	105	<0.5	0.24	5.2	2.4	45	<1	2370	27.8	55
Osor ore	31	0.008	>5000	<15	5.78	208	<3	74	<0.5	0.03	1.5	<0.5	15	<1	34,000	9	12
MgO	27	0.030	<3	<15	0.04	1.4	<3	83	<0.5	0.02	0.8	1.5	47	<1	6	<0.5	13
CAL *	1000	–	550	–	–	30	70	–	45	–	–	–	1000	–	1000	–	–

2.3. Mine Water, Mine Wastes, and MgO

Mine water was collected from the Coral adit, which drained the abandoned mine of Osor (Girona, NE Spain). The abandoned Osor mining area lies approximately 35 km SE of Girona, on the La Selva basin and Montseny-Guilleries massif, which belongs to the Catalonian Coastal Ranges (CCR) in the NE of the Iberian Peninsula. The main mine drainage was Coral adit, which drains the Osor vein system and had an estimated discharge in the Osor river varying between 800 and 1500 m^3/day of near-neutral contaminated mine water. Annually, mine water discharge was higher in the winter or spring, and lower, generally, in the late summer and early fall [5,45].

Mine waste at the study area consisted of flotation tailings and waste rock generated from the exploitation of the Osor vein deposit. Mineral deposits are located 4 km SE of the Anglés town, and they include several fluorite-barite-sphalerite-galena veins, exploited until 300 m of depth [5]. Gangue minerals included quartz, barite, calcite, pyrite, and silicates (mainly muscovite, albite, and biotite).

2.4. Column Leaching Experiments

The column leaching method was a modified PrEN 14,405 procedure, the standard European percolation test [46]. A column with the following dimensions was used: 750 mm long, 150 mm diameter, and 5 mm thick (Figure 1C). A 222 mm long plastic funnel with an internal diameter of 186 mm was attached to the bottom of the column. Inside the funnel, a fiberglass plate with holes in it acted as a support column. Methacrylate was coated onto a mesh that acted as a filter and retained the porous medium. The entire device was mounted on a metal structure to hold the column in a vertical position at a regular height above the surface. The contaminated mine water (GC sample) and the contaminated lixiviate (LT sample) used in the experiments were added in the column using a rain simulator connected to a metering pump, which provided a maximum flow of 10 L/h and could be adjusted from 1% to 100% of low-mineralized water (Figure 1C).

Contaminated mine water (GC sample) and tailings leachate (LT sample) percolated each column obtaining 6 samples of treated mine water: samples G-1 to G-6 (Tables 2 and 3) and six treated leachates (samples T-1 to T-6 in Tables 4 and 5). The samples were collected at the bottom of the column during 150 min at 0, 30, 60, 90, 120, and 150 min of the first effluent. The pH, redox potential (Eh; mV), water temperature, and electrical conductivity (EC; µS/cm) measurements were calibrated using standard solutions and measured in situ with portable devices (HACH model sensION TM378). The samples were filtered using a cellulose nitrate membrane with a pore size of 0.45 um. Samples for cation analysis were later acidified to pH < 2.0 by adding ultra-pure HNO_3. The samples were collected in 110 mL high-density polypropylene bottles, sealed with a double cap, and stored in a refrigerator until analysis.

Table 2. Composition of circum-neutral mine water and treated mine water samples. GC: mine water sample used in the column experiment. G-1 to G-6: treated mine water.

Analyte Symbol	Time	pH	Eh	EC	Mn	Fe	Co	Ni	Zn	Pb	As	Se	U	Mo	Cd	Sb	Cu
Unit	min	pH unit	mV	µS/cm	µg/L	µg/L	µg/L	µg/L	µg/L	µg/L	µg/L	µg/L	µg/L	µg/L	µg/L	µg/L	µg/L
Detection Limit					0.1	10	0.005	0.3	0.5	0.01	0.03	0.2	0.001	0.1	0.01	0.01	0.2
GC	—	7.46	98.6	678	841	120	19.1	17.9	2900	2.11	1.59	4.4	9.16	1.0	1.98	0.17	7.3
G-1	0	10.7	−750	7200	50.4	50	1.66	2.3	329	118	1.54	2.6	0.957	6.4	1.04	5.87	29.8
G-2	30	12.4	−725	4530	0.4	370	<0.005	0.5	8.2	1970	0.36	2.2	0.017	9.9	0.04	5.64	2.8
G-3	60	12.6	−776	6080	3.2	580	<0.03	<2	73.5	2470	0.34	1.4	0.104	7.1	0.06	13	4.9
G-4	90	12.6	−820	6470	0.9	550	<0.03	<2	76.5	1870	0.48	2.2	0.093	6.3	<0.05	12.9	6.1
G-5	120	12.7	−810	6730	2	630	<0.03	<2	69.5	1350	0.31	2	0.098	5.7	0.05	11.6	5.5
G-6	150	12.7	−750	6780	0.6	710	<0.03	<2	68.5	1000	0.4	1.8	0.081	5.4	<0.05	11.3	6

Table 3. Main anion contents of mine water (GC) and first and last treated mine water samples.

Analyte Symbol	Time	F	Cl	NO_3 (as N)	SO_4	HCO_3^-
Unit Symbol	min	mg/L	mg/L	mg/L	mg/L	mg/L
Detection Limit	—	0.01	0.03	0.01	0.03	1
GC	—	2.73	22.4	0.4	210.7	408
G-1	0	0.08	50.4	0.3	254.8	1222
G-6	150	0.2	30.1	0.1	123.3	3013

Table 4. Composition of untreated leached tailings (LT sample) and treated leachates (T-1 to T-6 samples).

Analyte Symbol	Time	pH	Eh	EC	Mn	Fe	Co	Ni	Zn	Pb	As	Se	U	Mo	Cd	Sb	Cu
Unit	min	pH unit	mV	uS/cm	µg/L	µg/L	µg/L	µg/L	µg/L	µg/L	µg/L	µg/L	µg/L	µg/L	µg/L	µg/L	µg/L
Detection Limit					0.1	10	0.005	0.3	0.5	0.01	0.03	0.2	0.001	0.1	0.01	0.01	0.2
LT	0	7.77	122	2420	80.9	830	1.85	3.8	2380	98.1	2.25	1.5	1.17	6.4	8.73	1.59	10.4
T-1	0	12.3	−700	4570	117	130	2.55	1.4	60.9	0.89	1.6	2.1	0.225	5.4	0.19	6.42	5
T-2	30	12.6	−678	5870	2.7	170	<0.03	<2	105	85.4	0.6	2.2	0.118	3.8	<0.05	12.1	3.4
T-3	60	12.6	−800	6400	<0.5	120	<0.03	<2	63.5	52.7	0.31	2.3	0.026	3.5	<0.05	12.8	1.9
T-4	90	12.6	−600	6700	<0.5	170	<0.03	<2	64.5	44.2	0.33	2	0.088	3.1	<0.05	12.9	2.8
T-5	120	12.7	−710	6860	<0.5	230	<0.03	<2	59.5	37.8	0.3	2.2	0.07	2.9	<0.05	13	2.7
T-6	150	12.7	−560	7030	<0.5	480	<0.03	<2	54	35.2	0.26	1.9	0.06	2.5	<0.05	14.4	2.6
MCL *	—-	—-	—-	—-	—-	—-	—-	120	1200	150	60	40	—-	200	20	100	600

(*) MCL: maximum contaminated level of solid waste leachates (percolation test) in order to deposit in landfills (inert solid waste).

Table 5. Main anion contents of untreated leached tailings (LT sample) and treated leachates (T-1 and T-6 samples).

Analyte Symbol	Time	F	Cl	NO_2 (as N)	Br	NO_3 (as N)	PO_4 (as P)	SO_4	HCO_3^-
Unit Symbol	min	mg/L	mg/L	mg/L	mg/L	mg/L	mg/L	mg/L	mg/L
Detection Limit	—	0.01	0.03	0.01	0.03	0.01	0.02	0.03	1
LT	0	2.3	36.4	0.33	<0.6	34.3	<0.4	1790	72
T-1	0	0.25	78.8	—	—	0.5	—	119.7	344
T-6	150	0.38	8.4	—	—	0.1	—	87.4	2950
MCL *	—	40	8500	—	—	—	—	7000	—

(*) MCL: maximum contaminated level of solid waste leachates (percolation test) in order to deposit in landfills (inert solid waste).

Metal concentrations were measured by inductively coupled plasma mass spectrometry (ICP-MS) at Actlabs (Ancaster, ON, Canada). Chloride, nitrate, and sulfate concentrations were analyzed in unfiltered samples by ion chromatography (IC). Water alkalinity was analyzed by titration. Standard reference material NIST 1640 (ICP-MS) was used to confirm accuracy. In order to preserve the carbonate equilibrium and CO_2 (g) levels in water samples, the samples collected for main anion determination were quickly closed and rapidly taken to the laboratory after sampling.

2.5. Geochemical Modeling

Hydrogeochemical analyses of leachates were performed using the PHREEQC [47] numerical code (version 3.0.6-7757) to evaluate the speciation of dissolved constituents and calculate the saturation state of the effluents. The MINTEQ thermodynamic database was used for chemical equilibrium calculations.

3. Results and Discussion

3.1. Mine Wastes and MgO

Chemical analysis of mine tailings revealed that Pb and Zn concentrations were above Catalonia's generic reference levels for human health protection applicable to soils

under industrial use (550 and 1000 mg/kg, respectively) (Table 1) [48]. Results from this analysis suggest that waste deposited in an open area is equivalent to contaminated soil, is inadequate for industrial use, and is susceptible to leaching, thus allowing the release of pollutants to surface water and groundwater. The bulk density and porosity of tailings were 1.291 and 0.22 g/cm^3, respectively, while the equivalent diameter obtained from grain size analysis was 1.5 mm.

The bulk composition of MgO is shown in Table 1. The calcium content was due to the presence of small amounts of dolomite, $MgCa(CO_3)_2$, in the natural magnesite. The presence of iron, aluminum, and silica did not interfere with the treatment of mine water and mine tailings, which remained inert in the reactive material. The elevated content of Cr and Ni may be associated to the grinding process of the natural magnesite. Porosity and equivalent diameter of MgO were 0.57 and 1.55 mm, respectively. The LG-MgO large particle size was necessary to establish a porosity that ensured the permeability of the medium.

3.2. Mine Water Treatment

The mine water sample used in the treatment (GC sample in Tables 2 and 3) showed high concentrations of Ca (167 mg/L), HCO_3 (408 mg/L), and SO_4 (210.7 mg/L) and a pH of 7.46, which might indicate calcite dissolution in the Coral adit. Additionally, the elevated concentrations of Mn (0.84 mg/L) and Zn (2.9 mg/L) suggest the dissolution of sphalerite and Mn oxides. Moreover, the mine water showed Na, Mg, and K concentrations above surface water and springs concentrations. The weathering of some detected silicates (albite and muscovite) might also explain the high pH detected [5].

A sharp increase in pH (from 7.46 to 12.75) can be observed when comparing samples collected from the column test (Tables 2 and 3) with the sample of mine drainage water. This could indicate that pH was controlled by the solubility of portlandite ($Ca(OH)_2$), formed by the rapid hydration reaction of the calcium dioxide present in the mixture of MgO [22].

In addition to pH, conductivity and redox potential markedly varied in the first post-treatment sample collected (G1) relative to the Coral gallery sample (GC). The initial EC in the contaminated water (less than 1000 µS/cm, GC sample) increased to over 7000 µS/cm, thus indicating a sharp rise in water mineralization, and decreased to 4530 µS/cm in sample G2, suggesting the progressive dissolution of some elements from the MgO substrate. The redox potential in the untreated Coral gallery sample was positive while the test samples presented values quite negative, which means that reduction reactions were favored over oxidation.

The main metal and metalloid concentrations in MgO-treated elutriates are listed in Tables 2 and 3. MgO was very effective in the removal of Cd (from 1.98 to <0.05 µg/L), Co (from 14.1 to <0.03 µg/L), F (from 2.73 to 0.2 mg/L), Mn (from 841 to 0.6 µg/L), Ni (from 17.9 to 0.5 µg/L), Si (from 9.3 to 0.3 mg/L), Ti (6.2 to <0.5 µg/L), U (from 9.16 to 0.08 µg/L), and Zn (from 2900 to 68.5 µg/L). Removal rates varied between 80% and 99%.

Other elements such as (from 1.59 to 0.31 µg/L) and Se (from 4.4 to 1.8 µg/L) presented a lower reduction in the last sample of the test compared to Coral gallery water. This indicates a reduced effectiveness of the treatment for these metals and metalloids when compared with others previously mentioned. Column tests using heavy metal contaminated waste showed that the degree of metal leaching was highly dependent on pH [49]. Increasing pH reduced the solubility of metals and metalloids. The presence of hydroxyl (OH^-) ions in aqueous solution and the negative Eh favored reduction reactions, which generated sparingly soluble metal compounds that precipitated in the solid matrix in the form of hydroxides, oxy-hydroxides, and carbonates [22].

These processes may explain removal rates observed for some of the metals analyzed after treatment with the MgO layer. Figure 2 shows the evolution of the concentration of major pollutants—Mn, Zn, Co, Ni, and U—during the column experiment. There was a sharp reduction in these five metals concentrations in the first collected sample (G1) compared with the untreated sample (GC). Concentrations continued to decrease in the

following 30 min (G2) increased at the 60 min mark (G3) and remained stable until the last sample was collected. The lower concentration changes of the sample relative to the G3-G2 evolution may be related to the decrease in EC (from 7200 to 4530 µS/cm) and the increase in pH (10.76 to 12.46) during the test as precipitation and other reactions occurred in the column experiment.

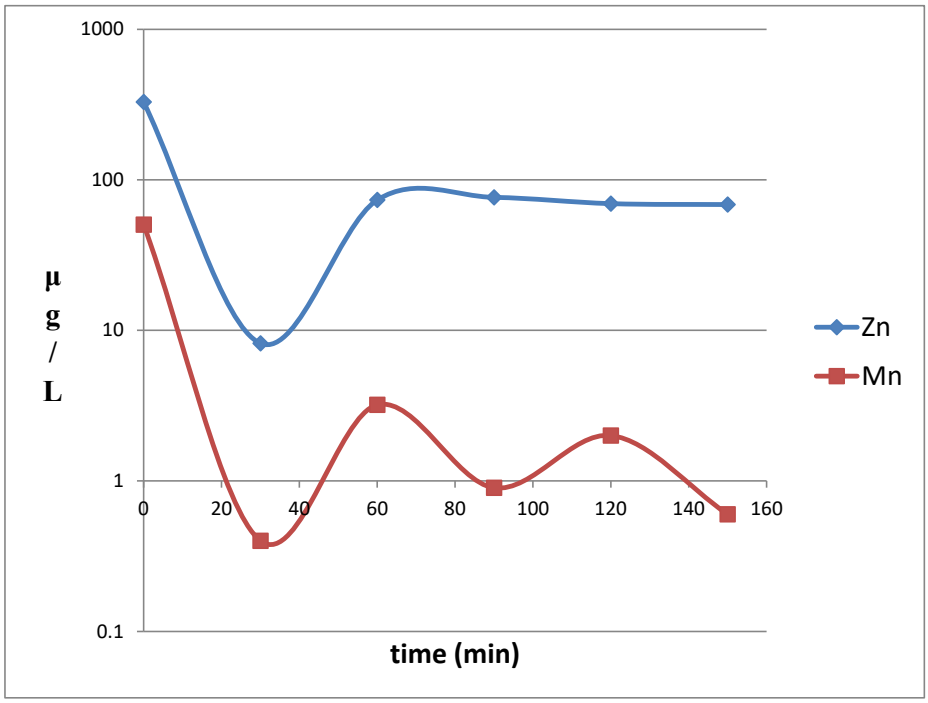

(**A**)

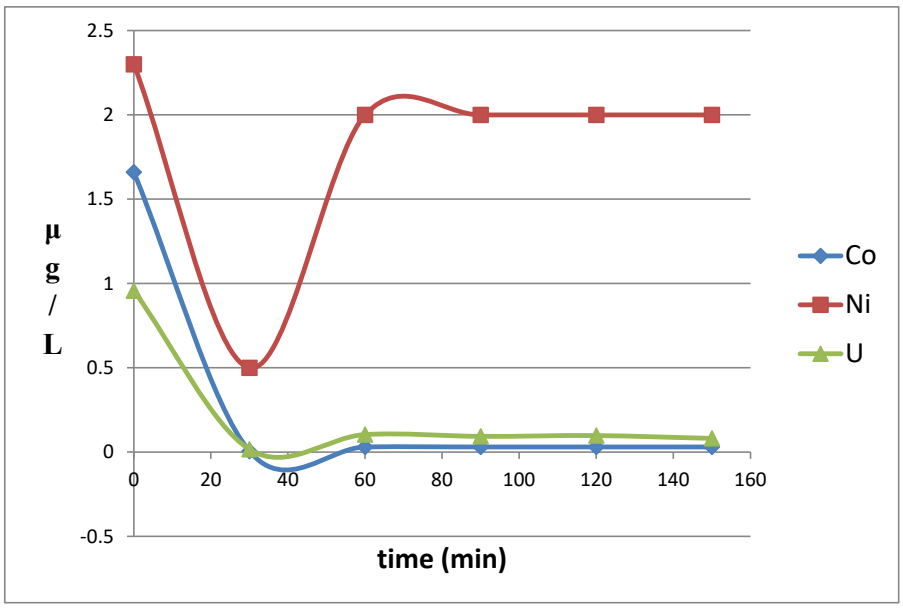

(**B**)

Figure 2. (**A**): Changes in Zn and Mn in the treating of mine water (GC sample) with MgO. (**B**): Changes in Co, Ni, and U in the treating of mine water (GC sample) with MgO.

The observed increase of Pb in the solution after the interaction with the MgO substrate may be explained by the change of solubility of lead hydroxide ($Pb(OH)_2$) as a function of pH. At a pH of about 9.5, the solubility of this compound is low. However, it increases significantly at pH values above 11 [49]. Studies using cement to stabilize Pb-rich wastes

also detected the increased release of Pb due to favorable conditions for generating the high alkalinity of the cement [50].

3.3. Treatment of Mine Tailings

Tables 4 and 5 and Figure 3 show the physicochemical parameters obtained in the leachates of the column experiment with flotation tailings and MgO (samples T-1 to T-6). The samples showed that pH varied between 12.3 and 12.7, Eh was always negative and ranged from −560 to −800 mV, and EC progressively increased throughout the experiment. The continuous decrease in concentrations during steady state flow indicates that metal contents in the leachate were controlled more by availability than by solubility of pure mineral phases [51]. The evolution of the main metals during the experiment showed a continuous decrease in concentration (Table 4). Results from leaching experiments also showed that Zn was the metal most released, with concentrations of 2.3 mg/L in tailings matching with the most abundant metal in waters. The concentration of Zn in pre-MgO treatment tailings (Figure 3) was above the maximum contaminant level for inert solid waste (1200 µg/L). Additionally, during MgO treatment there was a continuous decrease in Cd concentration (Table 5), with values below the maximum contaminant level (20 µg/L).

There was a continuous drop in Mn concentrations from 117.9 to less than 0.5 µg/L, while Fe increased from 130 to 480 µg/L, possibly because of the pH-Eh conditions of the experiment (Table 4, Figure 3). The leaching of Pb and Zn also showed an initial increase in concentrations in the sample collected at 30 min from the beginning of leaching (Figure 3). This phenomenon may be associated to an equilibrium process in column effluent during percolation and/or flow irregularities, which may produce increasing concentrations [51,52]. When comparing post-treatment concentration with metal and metalloid concentrations in untreated tailings (sample LT in Tables 4 and 5), we can see that the layer of MgO was very effective in removing As (from 2.25 to 0.26 µg/L), Cd (from 8.73 to <0.05 µg/L), Co (from 1.85 to <0.03 µg/L), F (from 2.3 to 0.38 mg/L), Mn (from 80.9 to <0.5 µg/L), Pb (from 98 to 35.2 µg/L), U (from 1.17 to 0.06 µg/L), and Zn (from 2380 to 54 µg/L). The reduction in metals and metalloids due to treatment was above 78%. Fe (from 830–480 µg/L). Mo (from 6.4 to 2.5 µg/L) and Cu (from 10.4 to 2.6 µg/L) showed a range of reduction between 50 and 78%, which indicates the efficacy of such a reactive layer.

3.4. Geochemical Modeling

Hydrogeochemical analyses of leachates were conducted to evaluate the speciation of dissolved constituents and to calculate the saturation state of the effluents (Tables 6 and 7). In addition, some pH-Eh diagrams were drawn using GWB [53]. The study of aqueous Cd speciation showed that the predominant species in treated leachates were $Cd(OH)_2$ and $CdCO_3$ (Table 6), which may indicate the mobilization of Cd if these species are stable in the pH-Eh conditions of the experiments. Mg speciation showed that $MgCO_3$ and Mg^{2+} are the predominant species, whereas Mn^{2+} and $Mn(OH)^{3-}$ were the most stable in Mn speciation. The geochemical speciation of Zn leachates indicates that Zn may be retained in the treated samples, although this metal may be mobilized as $Zn\ (CO_3)_2^{2-}$ and $Zn(OH)_4^{2-}$ in the MgO-treated samples.

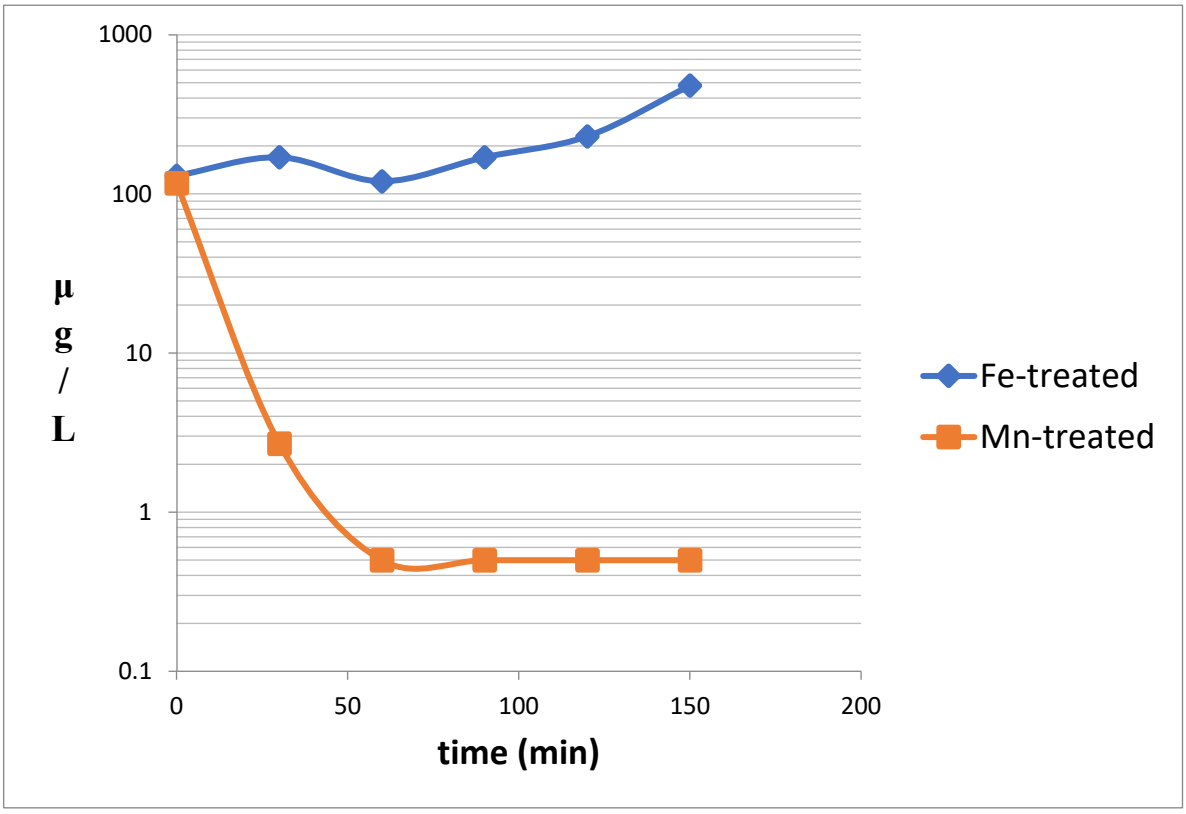

(**A**)

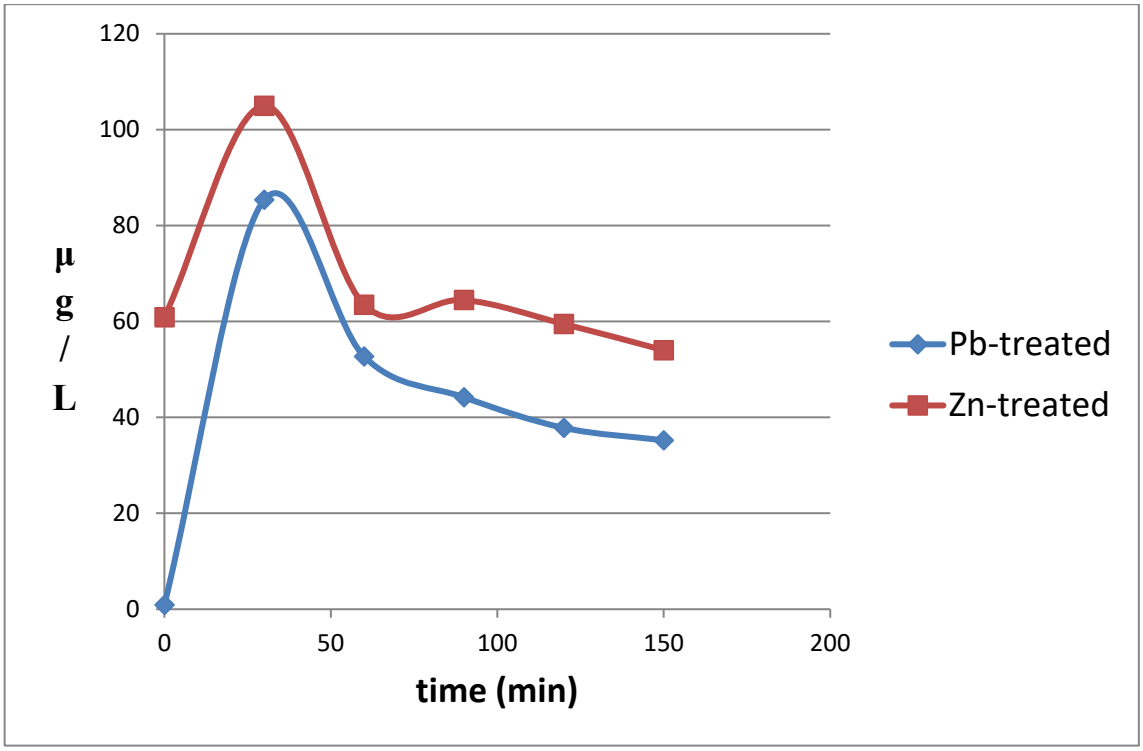

(**B**)

Figure 3. Treatment of mine tailing leachates. (**A**): Changes in Fe and Mn in the treatment of mine tailing leachates (LT sample) with MgO. (**B**): Changes in Pb and Zn in the treatment of mine tailing leachates (LT sample) with MgO.

Table 6. Distribution of species for leachates. Data calculated using PHREEQC and database Minteq. Values in molality.

Species	G-1	G-6	T-1	T-6
$CdCO_3$	8.16×10^{-9}	4.47×10^{-11}	2.01×10^{-11}	6.41×10^{-12}
$Cd(OH)_5$	1.66×10^{-10}	2.29×10^{-9}	1.26×10^{-9}	2.42×10^{-10}
$CdOH^+$	6.92×10^{-11}	1.10×10^{-11}	1.28×10^{-11}	1.18×10^{-12}
Cd^{2+}	2.48×10^{-11}	4.59×10^{-14}	1.15×10^{-13}	6.04×10^{-15}
$MgCO_3$	3.53×10^{-3}	1.47×10^{-6}	4.65×10^{-4}	3.83×10^{-7}
Mg^{2+}	2.42×10^{-3}	3.29×10^{-7}	6.53×10^{-4}	8.16×10^{-8}
$MgSO_4$	3.13×10^{-4}	9.68×10^{-9}	3.44×10^{-5}	1.75×10^{-9}
$MgHCO_3$	1.88×10^{-5}	1.61×10^{-6} *	1.51×10^{-3} *	3.58×10^{-7} *
Mn^{2+}	4.83×10^{-7}	7.40×10^{-12}	1.50×10^{-8}	8.53×10^{-12}
$MnOH^+$	4.3×10^{-7}	5.37×10^{-10}	5.36×10^{-7}	5.55×10^{-10}
$MnSO_4$	6.26×10^{-8}	2.05×10^{-13}	7.87×10^{-10}	1.74×10^{-13}
$MnHCO_3^+$	5.79×10^{-9}	1.04×10^{-8} **	1.58×10^{-6} **	8.57×10^{-9} **
$Zn(CO_3)_2^{-2}$	2.81×10^{-6}	5.94×10^{-11}	1.68×10^{-11}	7.68×10^{-11}
$Zn(OH)_2$	1.83×10^{-6}	1.52×10^{-8}	6.72×10^{-8}	1.46×10^{-8}
$Zn(OH)_3^-$	3.52×10^{-7}	3.57×10^{-7}	5.51×10^{-7}	3.04×10^{-7}
$ZnCO_3$	2.79×10^{-8}	6.79×10^{-7} ***	5.13×10^{-7} ***	5.10×10^{-7} ***

*: $MgOH^+$; **: $Mn(OH)_3^-$; ***: $Zn(OH)_4^{-2}$.

Table 7. Calculated saturation index for leachates. Saturation indices calculated using PHREEQC and database MINTEQ.

Species	GC	G-1	G-6	T-1	T-6
Artinite	−2.68	3.43	0.24	5.33	−1.05
Brucite	−2.70	1.80	1.85	4.45	1.15
$Cd(OH)_2$	−5.63	−3.16	−2.01	−2.27	−2.99
Chrysotile	2.44	13.69	5.80	16.20	3.89
Nesquehonite	−1.60	0.06	−3.18	−0.69	−3.77
Otavite	0.53	0.30	−1.98	−2.35	−2.84
Hydrozincite	39.79	35.12	17.90	20.87	18.04
Smithsonite	−0.55	−2.85	−8.35	−7.82	−8.25
Talc	3.79	12.95	−3.02	10.01	−4.72
$ZnCO_3{:}H_2O$	−0.21	−2.64	−8.09	−7.56	−7.99
Portlandite	−8.06	−4.89	−0.09	−0.86	−0.25

The PHREEQC calculations indicated that all leachates were saturated with respect to artinite (except leachate T-6), brucite, chrysotile, and hydrozincite (Table 7). Additionally, some leachates were saturated with respect to nesquehonite and talc (Table 7). According to the pH-Eh diagram (Figure 4), Mg first should precipitate as carbonate and/or brucite. Thus, metal removal in the treatment experiments could be associated first with the precipitation of brucite and metal hydroxides:

$$MgO + H_2O = 2OH^- + Mg^{2+} \quad (10)$$

$$2Mg^{2+} + 2OH^- = 2Mg(OH)_2 \quad (11)$$

$$M^{2+} + Mg(OH)_2 = M(OH)^{2+}\ Mg^{2+} \quad (12)$$

However, the pH-Eh conditions suggested that brucite may be an ephemeral phase and drive quickly to carbonation reactions producing the formation of magnesite and/or artinite and lansfordite/nesquehonite [33,54]. The carbonate species are formed as CO_2 dissolves in water [33,54]. Thus the main carbonation reactions may be:

$$Mg(OH)_2 + H_2O + H_2CO_3 \rightarrow MgCO_3{\cdot}3H_2O \text{ (nesquehonite)} \quad (13)$$

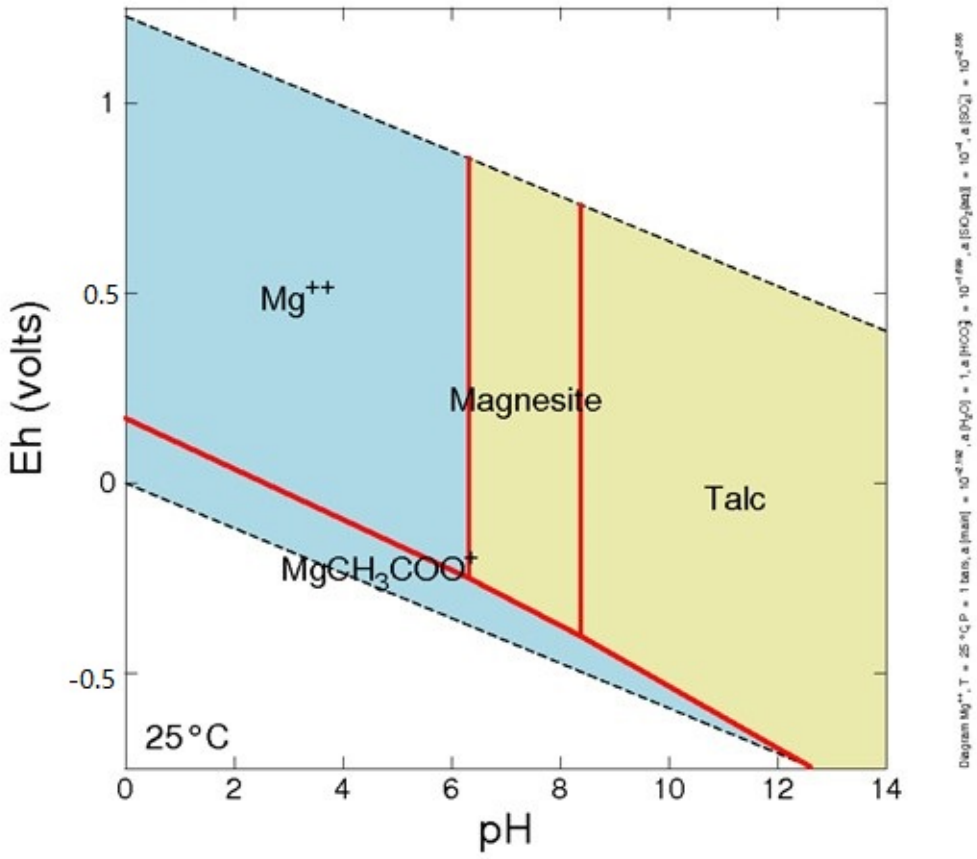

Figure 4. pH-Eh diagram for Mg.

Finally, with the pH increase (Figure 4), the hydration products: Talc ($Mg_3Si_4O_{10}(OH)_2$) and chrysotile ($MgSi_2O_5(OH)_4$) may be present [33] and might be partially responsible for the metal immobilization (Figure 4). Additionally, in similar MgO-based studies the presence of talc was detected by XRD analysis [33].

According to the pH-Eh conditions, Zn should be a low mobile element, especially under high pH (pH > 12) and slightly reducing conditions such as those of the MgO tests. Thus, Zn should be less mobile in alkaline and low redox environments due to the possible precipitation of zinc oxides and hydroxides. Additionally, geochemical modeling of leachates indicated that the most possible solid phase sink for Zn could be hydrozincite ($Zn_5(OH)_6(CO_3)_2$) since all the leachates showed super-saturation with respect to this mineral.

Divalent metals such as Mn, Cu, and Zn may be removed by adsorption and/or catalytic oxidation [55–59]. These metal removal mechanisms together with hydration products may be the main chemical processes related with the application of magnesium oxide in mine water treatment. Especially in the case of As, due to MgO, the adsorbent may exhibit a higher environmental stability [59].

4. Conclusions

MgO was tested as a reactive material in the removal of metals from mine water and mine waste leachate. Treatment performance was evaluated using column experiments and the PHREEQC numerical code. The use of MgO layer in the treatment of mine water was very effective in the removal of As (from 1.59 to 0.31 µg/L), Cd (from 1.98 to <0.05 µg/L), Co (from 14.1 to <0.03 µg/L), F (from 2.73 to 0.2 mg/L), Mn (from 841 to 0.6 µg/L), Ni (from 17.9 to 0.5 µg/L), U (from 9.16 to 0.08 µg/L), and Zn (from 2900 to 68.5 µg/L).

The treatment of leachates from Osor mining waste showed that the use of MgO was very effective in removing As (from 2.25 to 0.26 µg/L), Cd (from 8.73 to <0.05 µg/L), Co

(from 1.85 to <0.03 μg/L), F (from 2.3 to 0.38 mg/L), Mn (from 80.9 to <0.5 μg/L), Pb (from 98 to 35.2 μg/L), U (from 1.17 to 0.06 μg/L), and Zn (from 2380 to 54 μg/L).

Geochemical modeling showed that the mixing of MgO and contaminated water at environmental temperature may promote the formation of a stabilizing agent composed of carbonates and possible brucite. However, the pH-Eh conditions suggested that brucite may be an ephemeral phase and drive to carbonation reactions producing the formation of magnesite and/or artinite and lansfordite/nesquehonite. The carbonate species are formed as CO_2 dissolves in water.

Later, with the pH increase magnesium-silicate-hydrates (MSH) may remove Cd, Zn, and similar metals by sorption on MSH, substitution on the MSH lattice, and precipitation or co-precipitation with some of the hydrated phases. The pH-Eh experimental conditions suggested the possible formation of talc ($Mg_3Si_4O_{10}(OH)_2$).

Geochemical modeling of leachates indicated that the most possible solid phase sink for Zn would be hydrozincite ($Zn_5(OH)_6(CO_3)_2$) given that all the leachates showed supersaturation with respect to this mineral.

Divalent metals such as Mn, Cu, and Zn may be removed by adsorption and/or catalytic oxidation. These metal removal mechanisms, together with hydration products, may be the main chemical processes related to the application of magnesium oxide in mine water treatment.

Author Contributions: Investigation, M.I.M.d.M.; Writing—review & editing, A.N. All authors have read and agreed to the published version of the manuscript.

Funding: This research was funded by the Catalan Agency for the Administration of University and Research Grants (AGAUR), grant number SGR2009. Besides, the research was supported by the Consolidated Research Group on Economic and Environmental Geology and Hydrology (Universitat Politècnica de Catalunya-University of Barcelona).

Informed Consent Statement: Not applicable.

Conflicts of Interest: The authors declare no conflict of interest.

References

1. Al, T.A.; Martin, C.J.; Blowes, D.W. Carbonate-mineral/water interactions in sulfide-rich mine tailings. *Geochim. Cosmochim. Acta* **2000**, *64*, 3933–3948. [CrossRef]
2. Navarro, A.; Cardellach, E. Mobilization of Ag, Heavy metals and Eu from the waste deposit of Las Herrerías mine (Almería, SE Spain). *Environ. Geol.* **2009**, *56*, 1389–1404. [CrossRef]
3. Navarro, A.; Domènech, L.M. Arsenic and metal mobility from Au mine tailings in Rodalquilar (Almería, SE Spain). *Environ. Earth Sci.* **2010**, *60*, 121–138. [CrossRef]
4. Plante, B.; Benzaazoua, M.; Bussière, B. Predicting Geochemical Behaviour of Waste Rock with Low Acid Generating potential Using Laboratory Kinetic Tests. *Mine Water Environ.* **2011**, *30*, 2–21. [CrossRef]
5. Navarro, A.; Font, X.; Viladevall, M. Metal Mobilization and Zinc-Rich Circumneutral Mine Drainage from the Abandoned Mining Area of Osor (Girona, NE Spain). *Mine Water Environ.* **2015**, *34*, 329–342. [CrossRef]
6. MEND. *Review of Water Quality Issues in Neutral pH Drainage: Examples and Emerging Priorities for the Mining Industry in Canada*; MEND Report 10.1; MEND Initiative: Ottawa, ON, Canada, 2004.
7. Heikkinen, P.M.; Räisänen, M.L.; Johnson, R.H. Geochemical Characterization of Seepage and Drainage Water Quality from Two Sulphide Mine Tailings Impoundments: Acid Mine Drainage versus Neutral Mine Drainage. *Mine Water Environ.* **2009**, *28*, 30–49. [CrossRef]
8. Heikkinen, P.M.; Räisänen, M.L. Trace metal and as solid-phase speciation in sulphide mine tailings-Indicators of spatial distribution of sulphide oxidation in active tailings impoundments. *Appl. Geochem.* **2009**, *24*, 1224–1237. [CrossRef]
9. Navarro, A.; Martínez, F. Evaluation of Metal Attenuation from Mine Tailings in SE Spain (Sierra Almagrera): A Soil-Leaching Column Study. *Mine Water Environ.* **2010**, *29*, 53–67. [CrossRef]
10. Lottermoser, B. *Mine Wastes*, 3rd ed.; Springer: Berlin, Germany, 2010.
11. Appelo, C.A.J.; Postma, D. *Geochemistry, Groundwater and Pollution*, 2nd ed.; Balkema: Amsterdam, The Netherlands, 2010.
12. Younger, P.L.; Banwart, S.A.; Hedin, R.S. *Mine Water: Hydrology, Pollution, Remediation*; Kluwer Academic Publishers: Dordrecht, The Netherlands, 2002.
13. Wolkersdorfer, C. *Water Management at Abandoned Flooded Underground Mines*; Springer: Berlin, Germany, 2008.
14. Santos, S.; Machado, R.; Correia, M.J.N.; Carvalho, J.R. Treatment of acid mining waters. *Miner. Eng.* **2004**, *17*, 225–232. [CrossRef]

15. Othman, A.; Sulaiman, A.; Sulaiman, S.K. Carbide lime in acid mine drainage treatment. *J. Water Process Eng.* **2017**, *15*, 31–36. [CrossRef]
16. Gusek, J.J.; Figueroa, L.A. *Mitigation of Metal Mining Influenced Water*; Society for Mining Metallurgy, and Exploration, Inc.: Littelton, CO, USA, 2009; Volume 2.
17. PIRAMID. *Engineering Guidelines for the Passive Remediation of Acidic and/or Metalliferous Mine Drainage and Similar Wastewaters*; Piramid Consortium, Research Project of the European Commission 5th Framework Programma; PIRAMID Consortium; University of Newcastle Upon Tyne: Newcastle upon Tyne, UK, 2003.
18. Kaur, G.; Couperthwaite, S.J.; Hatton-Jones, B.W.; Millar, G.J. Alternative neutralization materials for acid mine drainage treatment. *J. Water Process Eng.* **2018**, *22*, 46–58. [CrossRef]
19. Nuttall, C.A.; Younger, P.L. Zinc removal from hard, circum-neutral mine waters using a novel closed-bed limestone reactor. *Water Res.* **2000**, *34*, 1262–1268. [CrossRef]
20. Mayes, W.M.; Potter, H.A.B.; Jarvis, A.P. Novel approach to zinc removal from circum-neutral mine waters using pelletized recovered hydrous ferric oxide. *J. Hazard. Mater.* **2009**, *162*, 512–520. [CrossRef] [PubMed]
21. U.S. Army Corps of Engineers. *Engineering and Design: Precipitation/Coagulation/Flocculation*; Manual EM 1110-1-4012; U.S. Army Corps of Engineers: Washington, DC, USA, 2001.
22. Navarro, A.; Chimenos, J.M.; Muntaner, D.; Fernández, I. Permeable reactive barriers for the removal of heavy metals: Lab-scale experiments with low-grade magnesium oxide. *Ground Water Monitor. Remed.* **2006**, *26*, 142–152. [CrossRef]
23. Navarro, A.; Cardellach, E.; Corbella, M. Immobilization of Cu, Pb, and Zn in mine-contaminated soils using reactive materials. *J. Hazard. Mater.* **2011**, *186*, 1576–1585. [CrossRef]
24. Bologo, V.; Maree, J.P.; Carlsson, F. Application of magnesium hydroxide and barium hydroxide for the removal of metals and sulphate from mine water. *Water SA* **2012**, *38*, 23–28. [CrossRef]
25. Siciliano, A. Removal of Cr (VI) from Water Using a New Reactive Material: Magnesium Oxide Supported Nanoscale Zero-Valent Iron. *Materials.* **2016**, *9*, 666. [CrossRef]
26. Jiang, D.; Yang, Y.; Huang, C.; Huang, M.; Chen, J.; Rao, T.; Ran, X. Removal of the heavy metal ion nickel (II) via an adsorption method using flower globular magnesium hydroxide. *J. Hazard. Mater.* **2019**, *373*, 131–140. [CrossRef]
27. Masindi, V.; Madzivire, G.; Tekere, M. Reclamation of water and the synthesis of gypsum and limestone from acid mine-drainage treatment process using a combination of pre-treated magnesite nanosheets, lime, and CO_2 bubbling. *Water Res. Ind.* **2018**, *20*, 1–14. [CrossRef]
28. Sulaiman, A.; Othman, A.; Ibrahim, I. The use of magnesium oxide in acid mine drainage treatment. *Mater. Today Proceed.* **2018**, *5*, 21566–21573. [CrossRef]
29. Kastyvehik, A.; Karam, A.; Aïder, M. Effectiveness of alkaline amendments in acid mine drainage remediation. *Environ. Technol. Innov.* **2016**, *6*, 49–59. [CrossRef]
30. Kim, T.Y.; Ahn, J.; Kim, C.; Choi, S.; Ho, T.T.; Moon, D.H.; Hwang, I. Carbonation/granulation of mine tailings using a MgO/ground-granule blast-furnace-slag binder. *J. Hazard. Mater.* **2019**, *378*, 120760. [CrossRef] [PubMed]
31. Jin, F.; Wang, F.; Al-Tabbaa, A. Three-year performance of in-situ solidified/stabilized soil using novel MgO-bearing binders. *Chemosphere* **2016**, *144*, 681–688. [CrossRef] [PubMed]
32. Li, W.; Ni, P.; Yi, Y. Comparison of reactive magnesia, quick lime, and ordinary Portland cement for stabilization/solidification of heavy metal-contaminated soils. *Sci. Total Environ.* **2019**, *671*, 741–753. [CrossRef]
33. Hwang, K.Y.; Seo, J.Y.; Phan, H.Q.H.; Ahn, J.Y.; Hwang, I. MgO-based binder for treating contaminated sediments: Characteristics of metal stabilization and mineral carbonation. *Clean Soil Air Water* **2014**, *42*, 355–363. [CrossRef]
34. Wang, L.; Chen, L.; Cho, D.; Tsang, D.C.W.; Yang, J.; Hou, D.; Baek, K.; Kua, H.W.; Poon, C. Novel synergy of Si-rich minerals and reactive MgO for stabilization/solidification of contaminated sediment. *J. Hazard. Mater.* **2019**, *365*, 695–706. [CrossRef]
35. Al-Zoubi, H.; Rieger, A.; Steinberger, P.; Pelz, W.; Haseneder, R.; Härtel, G. Optimization Study for Treatment of Acid Mine Drainage Using Membrane Technology. *Sep. Sci. Technol.* **2010**, *45*, 2004–2016. [CrossRef]
36. Wolkersdorfer, C.; Baierer, C. Improving Mine Water Quality by Low Density Sludge Storage in Flooded Underground Workings. *Mine Water Environ.* **2013**, *32*, 3–15. [CrossRef]
37. Noosai, N.; Vijayan, V.; Kengskool, K. Model application for acid mine drainage treatment processes. *Int. J. Energy Environ.* **2014**, *5*, 693–700.
38. Miller, A.; Figueroa, L.; Wildeman, T. Zinc and nickel removal in simulated limestone treatment of mining influenced water. *Appl. Geochem.* **2011**, *26*, 125–132. [CrossRef]
39. Madzivire, G.; Gitari, W.M.; Vadapalli, V.R.K.; Ojumu, T.V.; Petrik, L.F. Fate of sulphate removed during the treatment of circumneutral mine water and acid mine drainage with coal fly ash: Modelling and experimental approach. *Miner. Eng.* **2011**, *24*, 1467–1477. [CrossRef]
40. Masindi, V.; Gitari, M.W.; Tutu, H.; De Beer, M. Passive remediation of acid mine drainage using cryptocrystalline magnesite: A batch experimental and geochemical modeling approach. *Water SA* **2015**, *41*, 677–682. [CrossRef]
41. Weber, A.; Kassahun, A. How Geochemical Modeling Helps Understanding Processes in Mine Water Treatment Plants—Examples from Former Uranium Minin Sites in Germany. In Proceedings of the 13th International Mine Water Association Congress—"Mine Water & Circular Economy—A Green Congress", Lappeenranta, Finland, 25–30 June 2017.

42. Johnson, B.C.; Rohal, P.; Eary, T. Coupling PHREEQC with GoldSim for a more Dynamic Water Modeling Experience. In Proceedings of the MWD Conference: "Risk to Opportunity", Pretoria, South Africa, 10–14 September 2018.
43. Dube, G.M.; Novhe, O.; Ramasenya, K.; Van Zweel, N. Passive Treatment Technologies for the Treatmemnt of AMD From Abandoned Coal Mines, eMalahleni, South Africa-Column Experiments. *J. Ecol. Toxicol.* **2018**, *2*, 2–5.
44. Magagane, N.; Masindi, V.; Ramakkovhu, M.M.; Shongwe, M.B.; Muedi, K.L. Facile thermal activation of non-reactive cryptocrystalline magnesite and its application on the treatment of acid mine drainage. *J. Environ. Manag.* **2019**, *236*, 499–509. [CrossRef] [PubMed]
45. Bori, J.; Vallès, B.; Navarro, A.; Riva, M.C. Ecotoxicological risks of the abandoned F-Ba-Pb-Zn mining area of Osor (Spain). *Environ. Geochem. Health* **2017**, *39*, 665–679. [CrossRef] [PubMed]
46. SAIC. *An Assessment of Laboratory Leaching Tests for Predicting the Impacts of Fill Material on Ground Water and Surface Water Quality*; Toxic Cleanup Program; SAIC: Shanghai, China, 2003.
47. Parkhurst, D.L.; Appelo, C.A.J. *User's Guide to PHREEQC (Version 2)—A Computer Program for Speciation, Batch-Reaction, One-Dimensional Transport, and Inverse Geochemical Calculations*; USGS: Reston, VA, USA, 1999.
48. Agencia de Residus de Catalunya. *Nivels Genèrics de Referencia dels Elements Traça en Sòls a Catalunya per a la Protecció de la Salut Humana*; Generalitat de Catalunya: Barcelona, Spain, 2010.
49. Alpaslan, B.; Yukselen, M.A. Remediation of lead contaminated soils by stabilization/solidification. *Water Air Soil Pollut.* **2001**, *133*, 253–263. [CrossRef]
50. De Angelis, G.; Medici, F.; Montereali, M.R.; Pietrelli, L. Reuse of residues arising from lead batteries recycle: A feasibility study. *Waste Manag.* **2002**, *22*, 925–930. [CrossRef]
51. Wehrer, M.; Totsche, K.V. Effective rates of heavy metal release from alkaline wastes-Quantified by column outflow experiments and inverse simulations. *J. Contam. Hydrol.* **2008**, *101*, 53–66. [CrossRef]
52. Grathwohl, P. On equilibration of pore water in column leaching tests. *Waste Manag.* **2014**, *34*, 908–918. [CrossRef]
53. Bethke, C.M.; Yeakel, S. *The Geochemist´s Workbench Release 9.0, GWB Essentials Guide*; Aqueous Solutions LLC: Champaign, IL, USA, 2011.
54. Hay, R.; Celik, K. Accelerated carbonation of reactive magnesium oxide cement (RMC)-based composite with supercritical carbon dioxide ($scCO_2$). *J. Clean. Prod.* **2020**, *248*, 119282. [CrossRef]
55. Giro-Palma, J.; Formosa, J.; Chimenos, J.M. Stabilization Study of a Contaminated Soil with Metal(loid)s Adding Different Low-Grade MgO Degrees. *Sustainability* **2020**, *12*, 7340. [CrossRef]
56. Suzuki, T.; Nakamura, A.; Niinae, M.; Nakata, H.; Fujii, H.; Tasaka, Y. Lead immobilization in artificially contaminated kaolinite using magnesium oxide-based materials: Immobilization mechanisms and long-term evaluation. *Chem. Eng. J.* **2013**, *232*, 380–387. [CrossRef]
57. Jang, S.B.; Choong, C.E.; Pichiah, S.; Choi, J.Y.; Yoon, Y.; Choi, E.H.; Jang, M. In-situ growth of manganese oxide on self-assembled 3D-magnesium hydroxide coated on polyurethane: Catalytic oxidation mechanism and application for Mn(II) removal. *J. Hazard. Mater.* **2022**, *424*, 127267. [CrossRef] [PubMed]
58. Szymoniak, L.; Claveau-Mallet, D.; Haddad, M.; Barbeau, B. Application of Magnesium Oxide Media for Remineralization and Removal of Divalent Metals in Drinking Water Treatment: A Review. *Water* **2022**, *14*, 633. [CrossRef]
59. Sugita, H.; Oguma, T.; Hara, J.; Zhang, M.; Kawabe, Y. Effects of Silicic Acido n Leaching Behavior of Arsenic from Spent Magnesium-Based Adsorbents Containing Arsenite. *Sustainability* **2022**, *14*, 4236. [CrossRef]